Ultrasound Obstet Gynecol 2005; **25**: 12–18
Published online in Wiley InterScience (www.interscience.wiley.com). **DOI:** 10.1002/uog.1819

Ultrasound antenatal diagnosis of cleft palate by a new technique: the 3D 'reverse face' view

S. CAMPBELL*, C. LEES†, G. MOSCOSO‡ and P. HALL§

**Create Health Clinic, Harley Street and ‡National Heart and Lung Institute, Imperial College, London and †Divisions of Fetal–Maternal Medicine and §East of England Cleft Lip and Palate Service, Addenbrookes NHS Trust, Cambridge, UK*

KEYWORDS: 3D reverse face view; cleft lip; cleft palate; three-dimensional ultrasound

ABSTRACT

Objective *To assess the clinical value of a novel three-dimensional (3D) ultrasound technique, the reverse face view (3D RF view), in the antenatal categorization of facial clefting and in particular clefting of the hard palate.*

Methods *Eight cases of suspected orofacial clefting were examined by 3D surface rendering. The fetal lips and alveolar ridge were examined in the frontal plane and the face was then rotated through 180° on the vertical axis to examine the secondary palate by the 3D RF view.*

Results *In each case described, we were able to visualize the fetal face, lips and palate and make an antenatal diagnosis as to whether the palate was affected. In all cases, the antenatal diagnosis was subsequently confirmed. In one case with a left-sided cleft in the lips and alveolar ridge and an intact hard palate, the correct diagnosis was made but a cleft in the soft palate was missed.*

Conclusion *Although clefts of the lips and alveolar ridge are readily diagnosed on high-quality antenatal ultrasound, visualization of the fetal palate using existing techniques is unreliable. In the patients described here, the 3D RF technique allowed relatively straightforward assessment of the fetal palate with a high degree of accuracy. Copyright © 2004 ISUOG. Published by John Wiley & Sons, Ltd.*

INTRODUCTION

Orofacial clefting is among the most common of congenital abnormalities and its incidence is steadily rising. In Denmark the incidence rose from 1.45/1000 live births in 1942 to 1.89/1000 in 1981[1,2].

There are two distinct embryological pathways underlying the pathogenesis of facial clefts. A cleft of the lip (CL) is most commonly unilateral (UCL) and may be associated with a cleft of the ipsilateral alveolus (UCLA). Traditionally any cleft anterior to the incisive foramen, which might include the alveolus or just the lip, was termed a cleft (complete or incomplete) of the primary palate. This nomenclature is useful because it describes the commonly detected forms of cleft seen antenatally. However, a CL can be associated with a cleft of the secondary palate, i.e. that which passes posteriorly from the incisive foramen. This, which has a distinct mode of inheritance, would then be termed a complete unilateral cleft lip and palate (UCLP), or, if it occurs on both sides, bilateral cleft lip and palate (BCLP).

The embryological origins of clefts of the secondary palate appear to be distinct from those of clefts of the lip and alveolus. Isolated cleft palate (CP) is less common than is CLP; ultrasound studies almost certainly underestimate the incidence of isolated CP, as this condition is rarely diagnosed by ultrasound antenatally, and may not be identified immediately following delivery. In Denmark, isolated CP accounts for 25% of the total number of cases of facial clefts, but surveys in other countries show that the incidence varies; for example, it is over 50% in Northern Ireland[3] and Scotland[4] and 70–80% in the Faroe Islands and Greenland[5]. UCL can be complete, incomplete, lateral, bilateral and (rarely) medial and is due to a variety of failures of fusion of the maxillary swelling with the medial nasal process. Clefting of the secondary palate is always midline and is the result of failure of the palatine processes to elevate or grow. The secondary palate comprises the hard palate (immediately posterior to the incisive foramen) and the soft palate (posterior to the hard palate, containing no bone). A cleft of the hard palate must also affect the soft palate; however, it is possible for the soft palate to be cleft with the hard palate

Correspondence to: Prof S. Campbell, Create Health Clinic, 103–105 Harley Street, London W1G 6AJ, UK (e-mail: info@createhealth.org)
Accepted: 15 November 2004

remaining intact (previously termed an incomplete cleft of the secondary palate). These variations are illustrated in Figure 1, modified from the original more complex design by Kernohan[6].

The prognosis for UCL or UCLA without palatal involvement is also very different from that of CP, which is more commonly associated with difficulties of speech, hearing and feeding and (following surgery) mid-face protrusion. CP is twice as common in girls, while UCLP is twice as common in boys[2].

The incidence of structural abnormalities and syndromes associated with CLP ranges between 21%[7] and 38%[8]. The majority of cases are multifactorial, although a positive family history is obtained in about 26% of cases[9]. Therefore, prenatal diagnosis will rest primarily on careful screening with ultrasound. The effectiveness of ultrasound screening for CLP varies widely between series. Stoll *et al.*[10] described how a systematic approach improved the detection rate of facial clefts from 5.3% between 1979 and 1988 to 26.5% during the years 1989–1998. Nevertheless, the diagnosis of isolated CP is extremely low as a palatal defect will not be recognized on the standard oblique face view that is used routinely to assess the upper lip and alveolar ridge, because shadowing of the palate by the densely bony ridge makes visualisation difficult. Even though one's suspicion is raised once a diagnosis of UCL has been made, it is still extremely difficult to report on the state of the secondary palate with confidence, despite the introduction of three-dimensional (3D) technology[11].

A simple, rapid and effective technique to view the palate and assess its normality is required. We have previously described briefly and illustrated a new technique which we have termed the 3D 'reverse face' view (3D RF view)[12], which we postulated would be a simple, rapid and effective method of visualizing the palate and palatal defects. In this paper we describe our experience with the technique in the antenatal categorization of facial clefting (in particular palatal defects) in eight fetuses in which an initial two-dimensional (2D) diagnosis indicated the likelihood of a facial cleft.

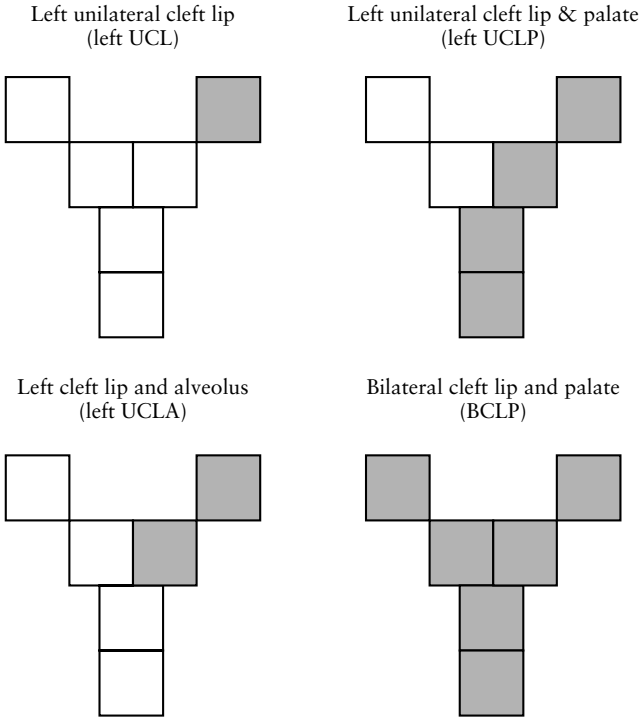

Figure 1 Diagram of Kernohan's 'striped Y', modified from the original more complex design[6].

METHODS

The ultrasound examinations in this investigation were performed with the GE Voluson 730 (GE Medical Systems, Bedford, UK) which has 2D, 3D, 4D and Doppler facilities. All ultrasound scans were undertaken by either one of two operators (S.C., C.L.), or both. The fetal face was visualized by obtaining a 2D profile or near-profile and the volume box adjusted to encompass the complete facial outline and cranium. To obtain a high-resolution 3D/4D image, a slow frame rate (2.7 Hz) or a 3D sweep was used. The harmonic setting was usually employed for better interface definition. Care was taken to avoid intervening limbs or umbilical cord obstructing the view of the lips and alveolus. The viewbar was adjusted to provide an optimized surface-rendered image of the face (Figure 2). If the face was oblique, it was rotated until a frontal view of the face was obtained. The lips were examined and the viewbar was then scrolled through the lips until the alveolar ridge was identified (Figure 3a). Further movement of the viewbar through the face to identify the palate usually resulted in a severely shadowed image which was diagnostically unhelpful and may be misleading (Figure 3b–d). The RF view overcame this problem. A return to the frontal view of the face was made and the face rotated through 180°. This provided an unobstructed view of the palatal area, nasal cavity and orbits. The viewbar was then scrolled through the length of the palate (Figure 4). It is important that a true coronal plane is obtained. This was ensured by minor adjustments to the rotational axis so that both eyes were symmetrically placed in the upper part of the image, with the nasal cavity in the midline between and just below the eyeballs. In normal cases, the intact palate was

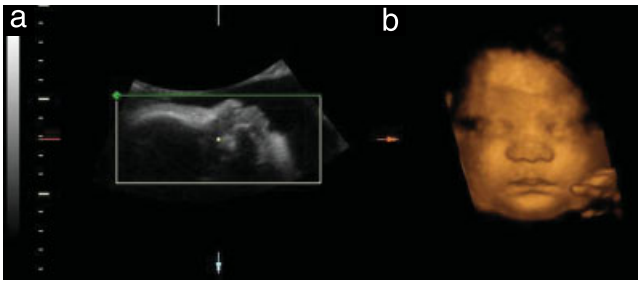

Figure 2 Demonstration of normal nose and lips. The viewbar is placed above a two-dimensional profile view of the face (a) to provide an optimal surface-rendered frontal image (b).

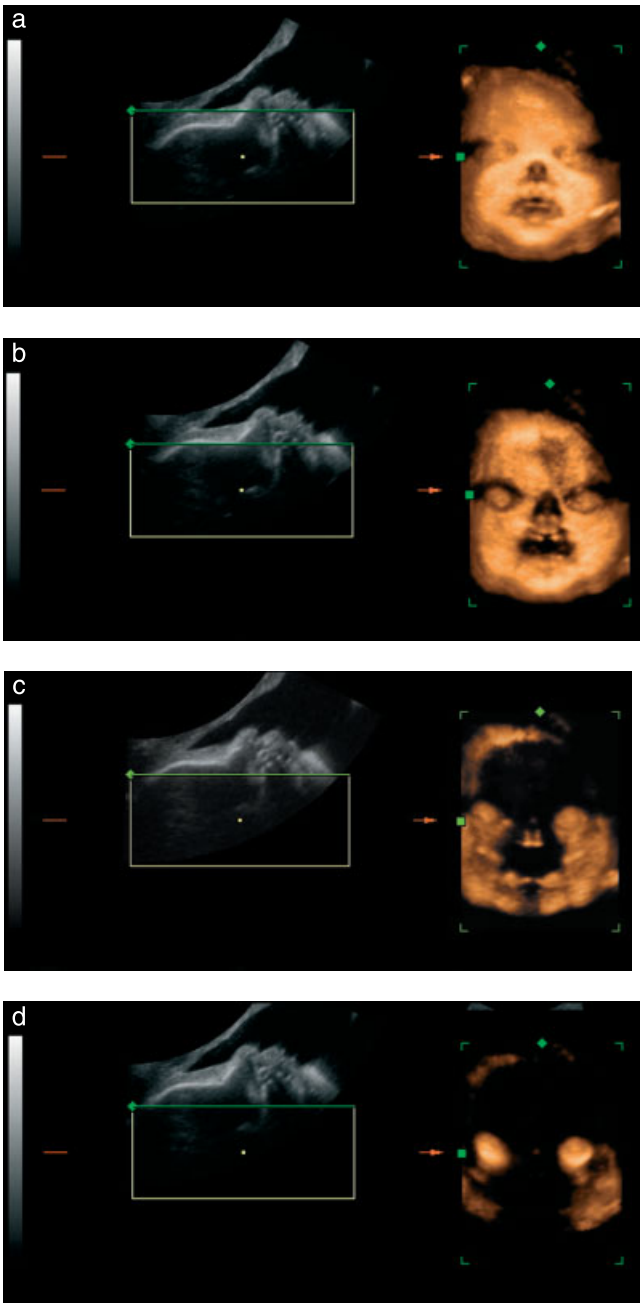

Figure 3 Sequential sections through the alveolar ridge and palatal area by the conventional front-to-back method. Beyond the alveolar ridge (a) there is increasing shadowing of the palatal area (b–d).

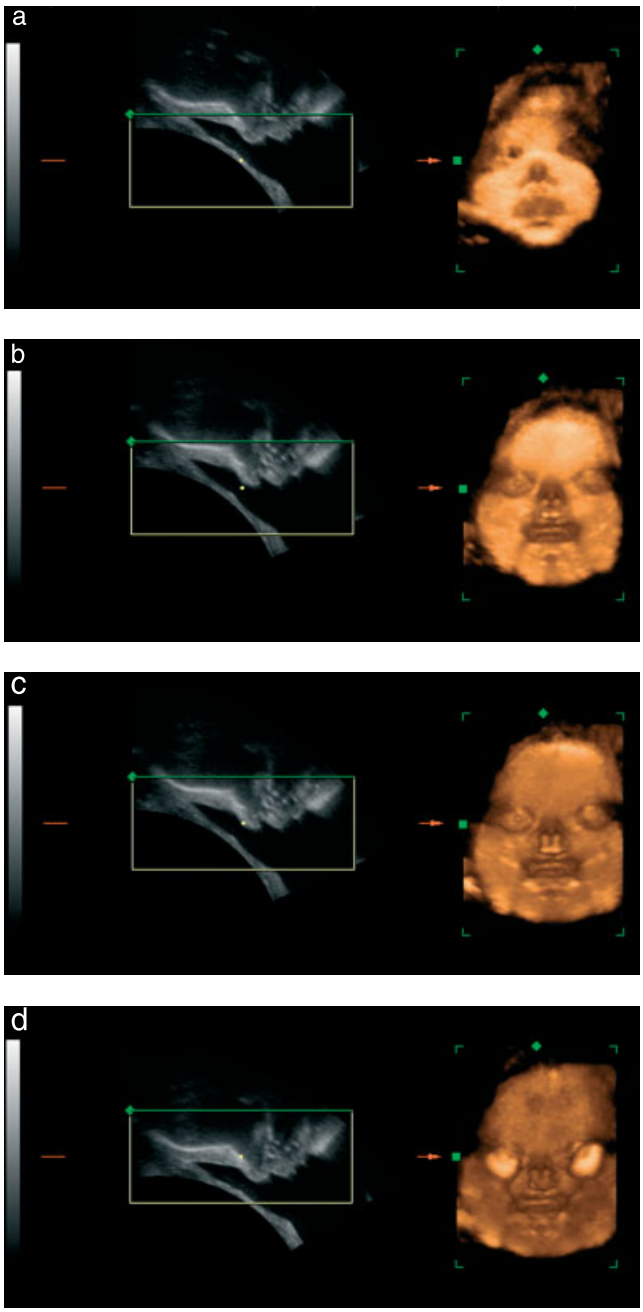

Figure 4 Images corresponding to those in Figure 3 showing the alveolar ridge and palate using the reverse face view. Clear visualization of the orbits, nasal cavity with septum and palate are identified at all levels from the alveolus (a) to the posterior aspect of the hard palate (b–d).

then seen as a distinct line separating the nasal from the oral cavities (Figure 5a). The hard palate could be clearly seen throughout its length, the only exception being when a limb in front of the face caused significant shadowing. This was usually only a temporary problem. Visualization of the hard palate, however, was not affected by umbilical cord or placenta. Degrees of obliquity of more than a three-quarter profile were unsuitable for obtaining a good RF view. The surface-rendered mode, in our experience, provided optimal visualization of the hard palate, although the gradient light algorithm also provided excellent views, especially of the bony palate and nasal cavity (Figure 5). We did not confidently identify the soft palate. This was probably due to the fact that the soft tissues of the velum do not provide sufficient reflections, although another factor is that as the velum hangs vertically down from the back of the hard palate, the plane of the soft palate is not at right angles in the coronal section.

The diagnosis and antenatal categorization of facial cleft was made in all eight cases by the RF view and these were all compared with detailed assessment after birth. The technique was rapid; obtaining the frontal view of the face to completion of visualization of the palate took 2 or

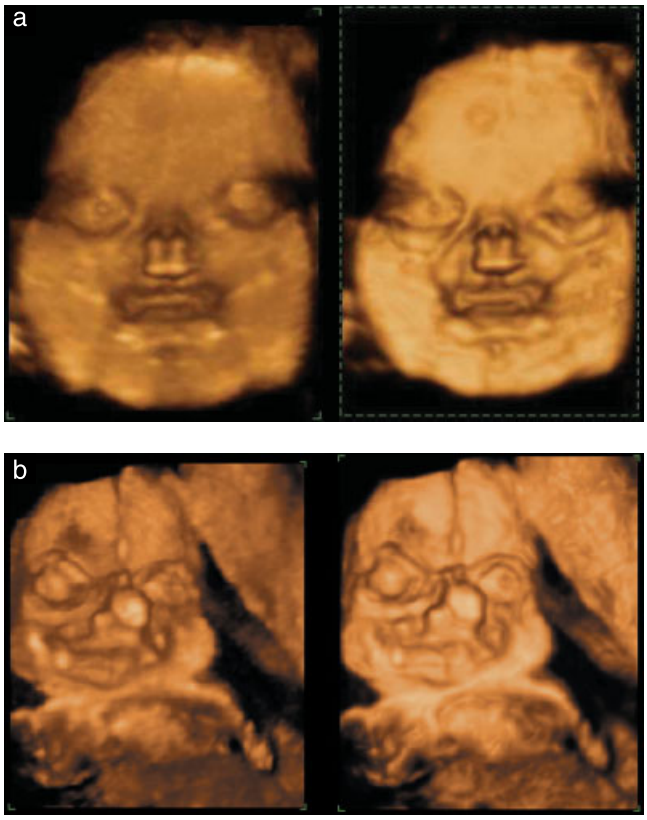

Figure 5 Ultrasound images comparing the palate using the three-dimensional reverse face view with conventional surface-rendered (left) and translucent light (right) algorithms. (a) Normal palate: the point of fusion of the two palatine shelves is seen clearly in the translucent light mode; at this stage (29 weeks' gestation) the point of fusion consists of a cartilaginous matrix. (b) Cleft palate in a 23-week fetus: the tongue protrusion through the defect is more clearly seen in the conventional surface-rendered view but the translucent light mode shows the bony defect with slightly better definition.

3 min. In all cases (except Case 8) the stored 3D volume was analyzed antenatally. In seven cases the categorization was made before the baby was born; in Case 8 the analysis of the 3D volume was made after the child was born but the analysis by one of us (S.C.) was done without prior knowledge of the postnatal findings. All women consented to ultrasound images being used in this study.

RESULTS

The diagnosis of facial cleft made in all eight cases by the RF view is illustrated here by a brief description of each case. Table 1 summarizes the pre- and postnatal findings. Case 1 has been described previously in a Picture of the Month article[12].

Case 1 was referred at 31 weeks because a scan 3 weeks previously at a tertiary center had diagnosed bilateral CL with major bilateral clefting of the alveolus. These findings were confirmed (Figure 6a). The RF view demonstrated a large defect in the primary and secondary (Figure 6b) palates. The edges of the cleft in the secondary palate were obscured by the tongue, which was partially elevated into the nasal cavity. The baby was born by spontaneous

Table 1 Comparison of prenatal diagnoses of clefts using the three-dimensional reverse face (3D RF) view with postnatal diagnosis in eight fetuses

Case	*Prenatal 3D RF diagnosis*	*Prenatal representation*	*Postnatal diagnosis*	*Postnatal representation*
1	BCLP		BCLP	
2	Left UCLP		Left UCLP	
3	Left UCLP		Left UCLP	
4	Left UCLP		BCLP	
5	Right UCLP		Right UCLP	
6	Left UCLP		Left UCLP	
7	Right UCLP		Right UCLP	
8	Left UCLA		Left UCLA + soft palate cleft	

BCLP, bilateral cleft lip and palate; UCLA, unilateral cleft lip and alveolus; UCLP, unilateral cleft lip and palate.

delivery at term + 4 days and weighed 3.27 kg. It had BCLP; the palatal defect was large. The CL was repaired 3 months after birth with partial closure of the hard palate, i.e. complete left vomerine flap, nasal floor reconstruction and a limited flap on the right side. The soft palate was repaired at 6 months of age.

Case 2 was referred at 29 weeks because a scan 5 weeks previously at a tertiary center had diagnosed left-sided CLA with deviation of the nasal septum. This was confirmed (Figure 7a). The RF view identified a narrow cleft of the secondary palate (Figure 7b). The baby was delivered spontaneously at 39 weeks and had UCLP. The CLA was repaired 3 months after birth and the CP 2 months after this.

Case 3 was referred at 25 weeks. A CL had been diagnosed during a routine scan at the local district

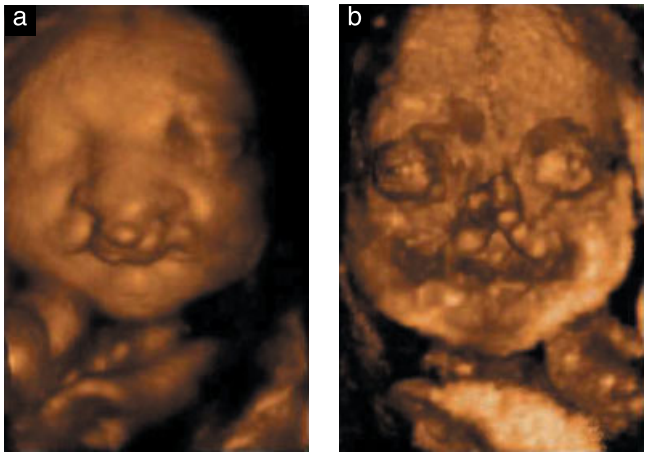

Figure 6 Ultrasound images of Case 1. (a) Frontal view demonstrating bilateral cleft lip. (b) Reverse face view demonstrating cleft in the secondary palate; the fetal tongue has a corrugated echogenic appearance and obscures the margins of the cleft.

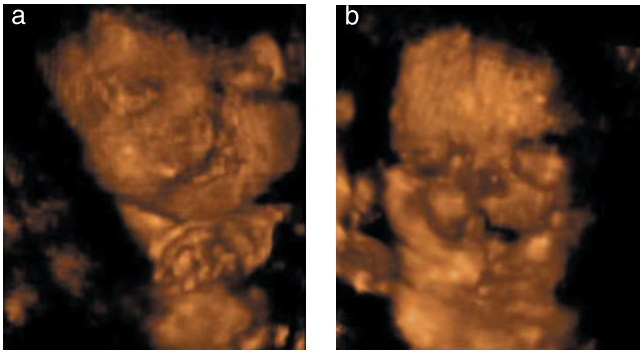

Figure 7 Ultrasound images of Case 2. (a) Frontal view showing left-sided cleft lip. (b) Reverse face view showing narrow cleft in the secondary palate.

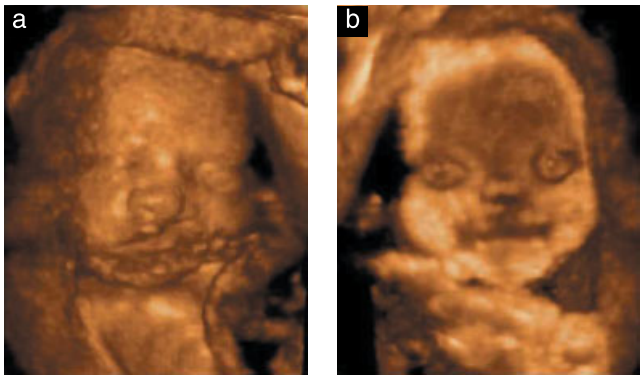

Figure 8 Ultrasound images of Case 3. (a) Frontal view showing left-sided cleft lip; the umbilical cord crosses the chin and left cheek. (b) Reverse face view showing a narrow cleft of the secondary palate.

hospital at 20 weeks. The local tertiary hospital diagnosed a left-sided CLA. This was confirmed (Figure 8a); the defect in the alveolar ridge measured 15.4 mm. The RF view showed a narrow cleft of the secondary palate (Figure 8b). The baby was delivered spontaneously at 40 weeks and weighed 3.6 kg. A left-sided CLA and CP were present. The CL was repaired at 10 weeks and the palatal repair was carried out 4 months after this.

Case 4 was referred at 23 weeks because left-sided CLA was diagnosed at a tertiary hospital on routine scanning at 20 weeks. The diagnosis was confirmed (Figure 9a) and at this time sonography could not exclude a right-sided CL. The RF view revealed a narrow clefting of the hard palate (Figure 9b). The baby was delivered spontaneously at 37 weeks and weighed 3.3 kg. A bilateral CL was present and there was also a defect in the secondary palate. The CL was repaired at 3 months and the palate was successfully closed at 6 months.

Case 5 was referred at 25 weeks because a CL had been diagnosed on routine scanning at a district hospital at 21 weeks. A right-sided CL (Figure 10a) was confirmed. The defect in the alveolar ridge measured 0.55 mm. The RF view demonstrated a large cleft of the secondary palate (Figure 10b). The baby girl was delivered by Cesarean section at 41 weeks and weighed 3.6 kg. A right-sided CL with a defect in the hard palate was confirmed. The cleft in the secondary palate was repaired 3 months after birth in a one/two-stage procedure.

Case 6 was referred at 31 weeks because a left-sided CLA had been diagnosed at a tertiary hospital. The lesion in the lip was thought to reach the nostril but did not distort the nasal structure. The diagnosis was confirmed (Figure 11a). The RF view identified a large defect in the secondary palate (Figure 11b). There was a large herniation of the fetal tongue through the defect into

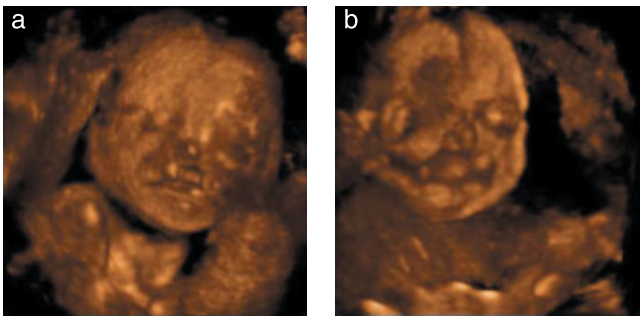

Figure 9 Ultrasound images of Case 4. (a) Frontal view showing left-sided cleft lip. (b) Reverse face view showing moderate clefting of the secondary palate.

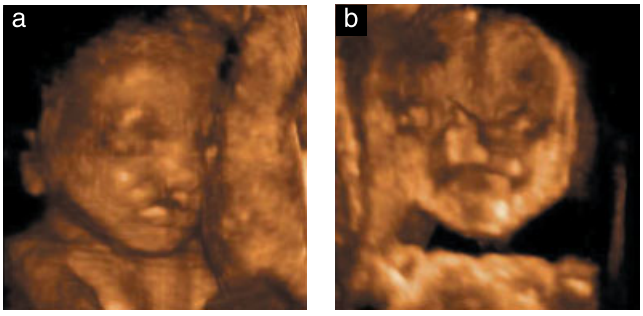

Figure 10 Ultrasound images of Case 5. (a) Oblique frontal view showing right-sided cleft lip. (b) Reverse face view demonstrating large cleft in the secondary palate.

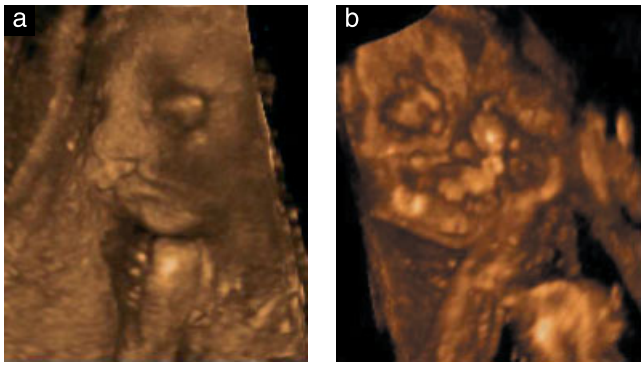

Figure 11 Ultrasound images of Case 6. (a) Oblique frontal view of left-sided cleft extending into the nose. (b) Reverse face view demonstrating large palatal defect; the fetal tongue is herniated into the nasal cavity and has the typical echogenic corrugated appearance.

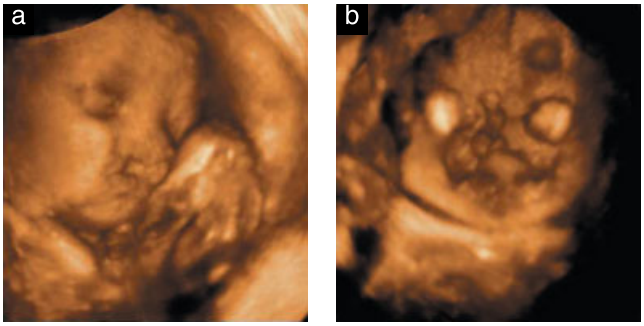

Figure 12 Ultrasound images of Case 7. (a) Oblique frontal view showing right-sided cleft lip. (b) Reverse face view showing large defect in the secondary palate.

the nasal cavity, obscuring the margins of the defect. The baby was delivered spontaneously at 40 weeks, and weighed 3.96 kg. A left-sided CLA with a large palatal defect was present. The CL was repaired 3 months after birth and the palate was repaired at 6 months.

Case 7 was referred at 28 weeks because a CL had been diagnosed on routine ultrasound at 22 weeks. A right-sided CL was identified (Figure 12a), and there was a defect in the alveolar ridge measuring 12 mm. The RF view identified a large defect in the secondary palate (Figure 12b). The baby was delivered spontaneously at 39 weeks. The ultrasound findings were confirmed. The CL was repaired 3 months after birth. A partial closure of the palatal defect was performed at 6 months and complete closure of the palate and alveolus will be completed at 6–7 years of age.

Case 8 was referred following a routine detailed scan at 20 weeks. A unilateral left-sided CL and alveolar ridge was noted on both 2D and 3D examinations. The 3D RF view was not analyzed until after the birth of the baby. The 3120-g baby underwent spontaneous vaginal delivery at 40 weeks. The child was noted to have a complete CL with a fissure in the alveolus. The hard palate was intact but there was an unpredicted cleft of the soft palate. There was a tiny 'notch' in the palpable posterior border of the hard palate. The baby therefore had an incomplete

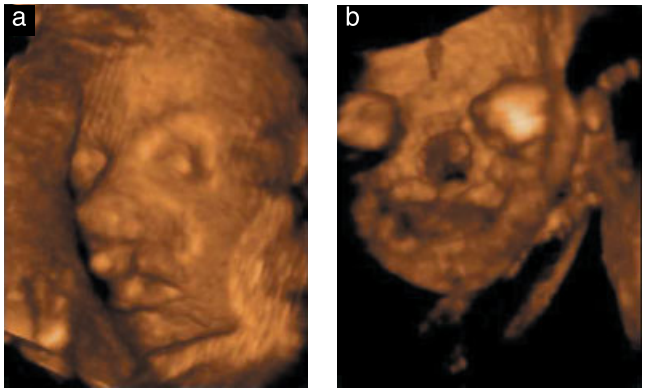

Figure 13 Ultrasound images of Case 8. (a) Oblique frontal view showing left-sided cleft lip. (b) Reverse face view showing intact secondary palate; the possible defect in the velum is visible.

cleft of the primary palate and an incomplete cleft of the secondary palate. Without knowledge of the postnatal findings analysis of the stored volume diagnosed left-sided clefting of the lip and alveolar ridge (Figure 13a) and an intact hard palate (Figure 13b). The cleft in the soft palate was not identified although subsequent analysis after knowledge of the postnatal findings did suggest a cleft of the velum.

DISCUSSION

At the present time high-resolution 2D scanning remains the cornerstone of prenatal diagnosis. The advantage of 3D over 2D imaging, apart from the apparent improvement in parental–fetal bonding and the increased facility to study fetal behavior[13], has been questioned. Nevertheless, new applications for 3D scanning are currently being explored in many centers as a result of the rapid improvement in equipment. 3D surface rendering has been used by several groups of workers to improve the diagnosis of CLP[14–19]. While most groups find that 3D improves the diagnostic capability of 2D ultrasound, one leading group found that 3D ultrasound failed to provide any additional diagnostic information[11].

On carefully reading these papers, both 2D and 3D images appear to illustrate clefts of the lips, alveolus and primary palate, but not of the secondary palate. The alveolus is clearly detectable on a 2D oblique face view and indeed 2D has the advantage that the size of the defect can be measured accurately. It is perhaps not surprising then that groups with experience in visualizing the alveolar ridge find that 3D does not confer any advantages, especially when, if it is applied in the conventional way, shadowing by the maxilla and alveolus remains problematical.

The 3D technique described here specifically overcomes the shadowing by rotating the frontal facial image through 180° along the vertical axis, so that the palate, nasal cavity and orbits can be approached from the reverse side. Why shadowing occurs when the viewbar is moved from the front backwards and not from the back forwards

defies rational explanation at the moment but in Figures 3 and 4 precisely corresponding views demonstrate that this happens. In over 300 studies between 18 and 34 weeks we have always been able to identify the fetal palate (unpubl. observ.). The method should be of value in determining palatal involvement when clefting of the lip and alveolus are diagnosed on 2D screening. It should also be of value in diagnosing isolated CP, as the technique is simple and rapid. However, as all the cases in this small series were referred specifically because of facial clefting as opposed to being detected during screening, further studies will have to be undertaken to evaluate the role of the RF view in the diagnosis of isolated CP.

There are still problems to be overcome in the diagnosis of CP by this technique. At present the Voluson 730 does not permit measurements to be made in the surface rendered modality, although a gross estimate (wide or narrow) can be made. Elevation of the tongue through the defect can also obscure the edges of the cleft, but the tongue is clearly identifiable as it is more echogenic than are surrounding tissues, and when protruding through the cleft it has a tortuous appearance. Any lesion associated with significant tongue elevation is certain to be large. It is also difficult at the present time to know whether defects of the velum (soft palate) can be identified. In Case 8, in a reassessment of the original diagnosis after the baby's birth, the appearance of a cleft posterior to an intact hard palate was seen. This may be over-interpretation, but further studies will determine whether clefting of the soft palate can be diagnosed with this method. Despite these problems, our experience suggests that surface rendering of intracranial structures using the 3D RF view can provide unique diagnostic information on the integrity of the secondary palate.

REFERENCES

1. Fog-Andersen P. *Inheritance of hare-lip and cleft palate*. Munksgaard: Copenhagen, 1943.
2. Jensen BL, Kreilborg S, Dahl E, Fogh-Andersen P. Cleft lip and palate in Denmark 1976–1981: Epidemiology, variability and early somatic development. *Cleft Palate Journal* 1988; **25**: 258–269.
3. Gregg T, Boyd D, Richardson A. The incidence of cleft lip and palate in Northern Ireland from 1980–1990. *Br J Orthod* 1994; **21**: 387–392.
4. Fitzpatrick DR, Raine PAM, Boorman JG. Facial clefts in the West of Scotland in the period 1980–1984: epidemiology and genetic diagnosis. *J Med Genet* 1994; **31**: 126–129.
5. Fog-Andersen P. Incidence and aetiology. In *Advances in the Management of Cleft Palate*, Edwards M, Watson ACH (eds). Churchill Livingstone: Edinburgh, 1980; 43–48.
6. Kernohan DA. The striped Y – a symbolic classification for cleft lips and palates. *Plast Reconstr Surg* 1971; **47**: 469.
7. Milerad J, Larson O, Hageberg C, Ideberg M. Associated malformations in infants with cleft lip and palate: a prospective, population- based study. *Paediatrics* 1997; **100**: 180–186.
8. Tolerova M, Cervenka J. Classification and birth prevalence of orofacial clefts. *Am J Med Genet* 1998; **75**(2): 126–137.
9. Hagberg C, Larson O, Milerad J. Incidence of cleft lip and palate and risks of additional malformations. *Cleft Palate Craniofac J* 1998; **35**: 40–45.
10. Stoll C, Dott B, Alembic Y, Roth MP. Evaluation of prenatal diagnosis of cleft lip/palate by foetal ultrasonographic examination. *Ann Genet* 2000; **43**: 11–14.
11. Ghi T, Perolo A, Banzi C, Contratti G, Valeri B, Savelli L, Morselli GP, Bovicelli L, Pilu G. Two-dimensional ultrasound is accurate in the diagnosis of fetal craniofacial malformation. *Ultrasound Obstet Gynecol* 2002; **19**: 543–551.
12. Campbell S, Lees CC. The three-dimensional reverse face (3D RF) view for the diagnosis of cleft palate. *Ultrasound Obstet Gynecol* 2003; **22**: 552–554.
13. Campbell S. 4D or not 4D: that is the question. *Ultrasound Obstet Gynecol* 2002; **19**: 1–4.
14. Merz E, Bahlmann F, Weber G, Macchiella D. Three-dimensional ultrasonography in prenatal diagnosis. *J Perinat Med* 1995; **23**: 213–222.
15. Chen ML, Chang CH, Yu CH, Cheng YC, Chang FM. Prenatal diagnosis of cleft palate by three-dimensional ultrasound. *Ultrasound Med Biol* 2001; **27**: 1017–1023.
16. Lee W, Kirk JS, Shaheen KW, Hodges AN, Comstock CH. Fetal cleft lip and palate detection by three-dimensional ultrasonography. *Ultrasound Obstet Gynecol* 2000; **16**: 299–301.
17. Johnson DD, Pretorius DM, Budorick NE, Jones NE, Jones MC, Lou KV, James GM, Nelson TR. Fetal lip and primary palate; three-dimensional ultrasound. *Radiology* 2000; **217**: 236–239.
18. Shipp TD, Mullikan JB, Bromley B, Benacerraf B. Three-dimensional prenatal diagnosis of frontonasal malformation and unilateral cleft lip/palate. *Ultrasound Obstet Gynecol* 2002; **20**: 290–293.
19. Chmait R, Pretorius D, Jones M, Hull A, James G, Nelson T, Moore T. Prenatal evaluation of facial clefts with two dimensional and adjunctive three dimensional ultrasonography: a prospective trial. *Am J Obstet Gynecol* 2002; **187**: 946–949.